Available online at **www.joac.info**

ISSN: 2278-1862

Journal of Applicable Chemistry

2020, 9 (4): 638-648

(International Peer Reviewed Journal)

A Computational Study of Homolytic Bond Dissociation Process Involved in the Initiation Process of Atom Transfer Radical Polymerization

Chetana Deoghare*

Department of Chemistry, Indus Institute of Sciences, Humanities and Liberal Studies,
Indus University, Rancharda, via Thaltej, Ahmedabad - 382115, Gujarat, **INDIA**
Email:chetanadeoghare.gd@indusuni.ac.in

Accepted on 11th July, 2020

ABSTRACT

This paper presents a computational study on homolytic bond dissociation of a number of alkyl halides R–X (R = succinimide, ethyl-isobutyrate, X = Cl, Br, I) which can be potential initiators for the atom transfer radical polymerization (ATRP). The density functional theory with B3LYP functional and 6-31+G(d)/LanL2DZ basis sets is used in the prediction of geometries and energetics associated with the dissociation of R-X bond. The relative equilibrium constant for the ATRP activation/deactivation process is calculated from the free energy values, and its variation with system parameters (such as solvent, temperature and substituent) is investigated. Comparison with the known initiators for the ATRP shows that some of the studied compounds have potential to initiate the ATRP process.

Graphical Abstract

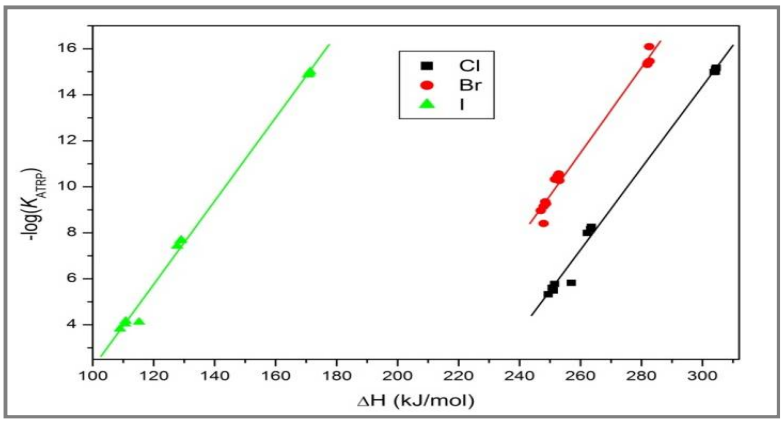

Correlation plot of relative K_{ATRP} values with R–X bond enthalpies of studied alkyl halides.

Keywords: Density functional theory (DFT), Bond dissociation energy, Homolysis, ATRP.

INTRODUCTION

Atom transfer radical polymerization (ATRP) [1-4] is one of the popular and robust controlled radical polymerization (CRP) technique [5, 6] and has been used for the preparation of polymers with controlled architecture and site specific functionality [7, 8]. Like other CRP methods [9-11], ATRP is controlled by equilibrium between propagating radicals and dormant species (mostly in the form of initiating alkyl halides R–X or macromolecular species). The basic mechanism of ATRP process (Scheme 1) involves homolytic cleavage of alkyl halide (R–X) bond (activation step) by a transition metal complex in its lower oxidation state (the activator, M_t^nY/L) generating (with rate constant of activation k_{act}) reversibly the propagating radical ($R^{\bullet}$) and the transition metal halide complex in its higher oxidation state (the deactivator, $X–M_t^{n+1}Y/L$) [12, 13]. In the deactivation step (with rate constant of deactivation k_{deact}), the halide atom X is transferred back from the activator to the propagating radical, also through homolytic bond dissociation. Similar to conventional radical polymerization, polymer chains grow by the addition of the intermediate radicals to the monomer (with rate constant of propagation k_p), or terminate (with rate constant of termination k_t) by radical coupling or disproportionation. However, only a few percent of the polymer chain undergoes termination in ATRP [12, 13].

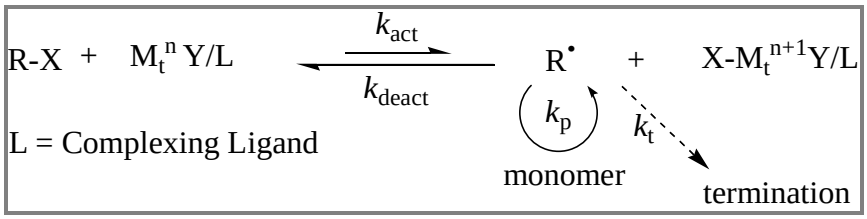

Scheme 1. Mechanism of Transition-Metal-Catalyzed ATRP.

The rate of an ATRP process depends on the rate constant of propagation and the concentration of monomer and propagating radical [8]. The radical concentration depends on the position of the equilibrium ($K_{ATRP} = k_{act}/k_{deact}$) and hence K_{ATRP} plays an important role in controlling the ATRP process. Thus, knowledge of K_{ATRP} and its dependence on system parameters, e.g. the structure of alkyl halides (initiator/dormant species), structure of catalyst (nature of metal ion, structure of the ligand), and the reaction conditions (solvent, temperature, etc.) is very important to understand an ATRP process [13]. Several experimental studies [14-19] have reported the kinetic and thermodynamic parameters of ATRP. Alternatively, there have been substantial progress in the application of quantum chemistry to radical polymerization processes in recent years and quantum-chemical methods have been applied successfully to study kinetics and thermodynamics of ATRP process [20, 21]. There exist two general methods for determination of K_{ATRP}, viz. (a) from the polymerization kinetics in presence of excess $X–M_t^{n+1}Y/L$, [15, 22] and (b) using Fischer-Fukuda equation of persistent radical effect [23, 24], or its variant [16]. Alternatively, relative values of K_{ATRP} can be estimated from the homolytic bond dissociation energy (BDE) of R–X under certain conditions [25-29]. Though, experimental data on BDEs for alkyl halides relevant for ATRP are limited, the energetics of bond dissociation can be accessed computationally using, for example density functional theory. As K_{ATRP} depends heavily on nature of alkyl halide and the catalyst used, the atom transfer equilibrium of ATRP process,

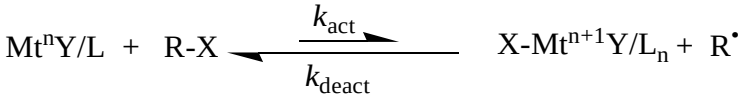

can be viewed [13] as sum of the following two equilibrium processes, viz. (i) homolytic bond dissociation of alkyl halide, (ii) $X–M_t^{n+1}Y/L$ bond formation (*halidophilicity*), so that $K_{ATRP} = k_{act}/k_{deact} = K_{RX} \times K_X$.

$$\text{(i)}\quad \text{R-X} \underset{}{\overset{K_{RX}}{\rightleftharpoons}} \text{R}^{\bullet} + \text{X}^{\bullet}$$

$$\text{(ii)}\quad \text{Mt}^{n}\text{Y/L} + \text{X}^{\bullet} \overset{K_{X}}{\rightleftharpoons} \text{Mt}^{n+1}\text{YX/L}$$

The value of the equilibrium constant K_X depends on the type of catalyst/ligand (M_t^nY/L) and halogen X. For similar conditions and using the same catalytic system (similar K_X), the overall equilibrium constant K_{ATRP} will depend on the energetics of alkyl halide R–X. In this situation, knowledge of the equilibrium constant K_{RX} alone will enable one to predict the relative values of *K*ATRP [**13, 25, 26**].

A lot of research has been carried out towards the copolymerization of variety of monomers and resulting polymers are obtained with useful applications [**30-33**]. The copolymerization of imides (such as *N*-arylitaconimides) with methyl methacrylate (MMA) is interesting to study, because, the incorporation of imides in the polymer backbone enhances the glass transition temperature and thermal stability of resulting polymers [**34, 35**]. However, the conventional radical polymerization of the chosen monomers reported in literature, offers poor control over the molecular weight and polydispersity of the resulting polymers [**34, 35**]. Recently, the ATRP method for the copolymerizations of various *N*-arylitaconimide with MMA (in anisole at 80°C and CuBr/bipyridine as catalyst) has been reported [**36**]. The commercially available initiator, ethyl-α-bromoisobutyrate (EtBiB), which resembles one of the monomers (MMA) has been used in our previous study [**36**]. It will be of interest to copolymerize the same system with different initiators having structural similarities with the other monomer (the itaconimide) and can be prepared from renewable resources. In view of this, some of model alkyl halides having structural similarities of substituted itaconimides have been investigated using density functional theory (DFT) before attempting them as initiators for the ATRP copolymerization. The aim of this study, is to find the homolytic bond dissociation energies, estimate the relative value of the equilibrium constant K_{ATRP}, study their variations with system parameters for these alkyl halides and to identify their potential as initiators for the ATRP process.

MATERIALS AND METHODS

The bond dissociation enthalpies (BDEs) and other energetics for the four series of alkyl halides 1, 2, 3 and 4 (Figure 1) in gas phase as well as in presence of two polar solvents (anisole and acetonitrile) at two different temperatures (25°C and 80°C) using density functional theory have been studied. The chosen test set of alkyl halides includes common ATRP initiators (Figure 1, Series 4) as well as species that mimic the dormant chain ends in the polymerization of *N*-phenylitaconimide (PI) and MMA (Figure 1, Series 1-3). The effect of their structure (e.g. primary, secondary and tertiary alkyl halides), different substituent's, medium, and temperature on the C–X bond dissociation is studied and the comparison of their performance with known potential initiators is evaluated.

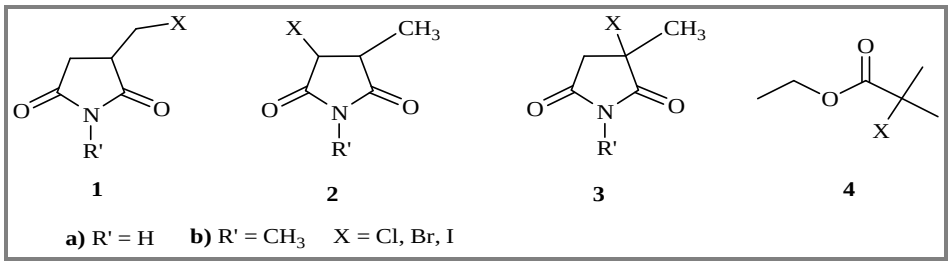

Figure 1.The alkyl halides **1** (**1a**-X to **1b**-X), **2** (**2a**-X to **2b**-X), **3** (**3a**-X to **3b**-X) and **4**-X, (X = Cl, Br, I) investigated in this study.

Computational Details: Gaussian09 [37] was used as source program for all calculations. All the geometries were fully optimized using the hybrid B3LYP exchange correlation functional [38-40] with 6-31+G(d) basis set, except for Iodine, where the LanL2DZ basis set is used. Frequency calculations were performed for all the compounds to check (no imaginary frequencies) the stationary points as minima on the potential energy surface. Systems containing unpaired electrons were optimized with spin unrestricted formalism. The spin contamination was found to be negligible (the mean value of the S^2 operator was close to the theoretical value of 0.75 for all radicals). A spin-orbit correction term was applied for X = Cl, Br and I due to their atomic nature. As the DFT calculation includes only the average energy of the ground state ^2P term, the extra stability of the real ground-state $^2P_{3/2}$ term is taken from the literature values [41] (0.8, 3.5 and 7.3 kcal/mol for Cl, Br and I respectively). Solvent effects are studied using Tomasi's polarizable continuum model (PCM) [42].

RESULTS AND DISCUSSION

DFT method was used to calculate BDEs as the difference of energy of R–X and energies of separated R and X radicals. This level of theory has been used in the literature for studying similar processes [12, 13]. The C–X bond lengths, BDEs and other energetics results for the studied alkyl halides, both in the gas phase and in two common organic solvents (anisole and acetonitrile) at two different temperatures, are displayed in table 1-3.

Structural Features of Alkyl Halides and Alkyl Radicals: The C–X bond distances for the studied compounds are given in table 1. They are between the ranges 1.81Å to 2.20Å for series **1**, 1.82Å to 2.22Å for series **2**, 1.84Å to 2.26Å for series **3** and 1.86Å to 2.28Å for the series 4 halides. It follows the trends 1 < 2 < 3 < 4 for a given X, and Cl < Br < I for a given series. The C–X bond lengths systematically increases for all the studied halides with increasing polarity of the medium and follow the trends gas phase < anisole < acetonitrile for a given RX. The dihedral angles for the C–X bond with respect to the ring (or with respect to $C(O)OC_2H_5$ for 4) are between 74°–84° for series 1 and 4, between 98°–108° for series 2 and 3. The carbon atom bearing the unpaired electron for all the radicals are found to be planar in the sense that the sum of the three bond angles at this carbon are found to be 360° in all cases. The spin densities at this carbon varies from 0.8 to 1.2 in the order 1 > 2 > 3 ≈ 4.

Table 1. The C–X bond length of studied alkyl halides in gas phase and in solution phase

R-X	r_{c-x} (Å)		
	Gas phase	Anisole	Acetonitrile
1a-Cl	1.808	1.817	1.822
1a-Br	1.965	1.973	1.977
1a-I	2.202	2.21	2.214
1b-Cl	1.809	1.817	1.822
1b-Br	1.966	1.974	1.978
1b-I	2.203	2.21	2.214
2a-Cl	1.818	1.822	1.823
2a-Br	1.976	1.98	1.981
2a-I	2.223	2.225	2.227
2b-Cl	1.82	1.824	1.826
2b-Br	1.977	1.981	1.982
2b-I	2.224	2.226	2.228
3a-Cl	1.84	1.845	1.848
3a-Br	2.007	2.012	2.015
3a-I	2.259	2.265	2.268
3b-Cl	1.843	1.847	1.85
3b-Br	2.008	2.013	2.016
3b-I	2.261	2.265	2.267
4-Cl	1.855	1.865	1.869
4-Br	2.017	2.025	2.029
4-I	2.278	2.287	2.292

Homolytic Bond Dissociation Enthalpies and Free Energies: The bond dissociation enthalpy (BDE) data for the studied compounds is displayed in table 2. They are in the ranges 304.26 kJ mol^{-1} to 170.34 kJ mol^{-1} for series 1, 264.55 kJ mol^{-1} to 129.98 kJ mol^{-1} for series 2, 252.37 kJ mol^{-1} to 110.83 kJ mol^{-1} for series 3 and 257.07 kJ mol^{-1} to 115.16 kJ mol^{-1} for the series 4 alkyl halides. The R–X homolytic BDEs of alkyl chlorides are found to be higher than the corresponding bromides, which are in turn higher than their iodide counterparts. This variation is parallel to the decreasing ionic character of halides, Cl > Br > I. The decrease in BDEs are about 10–25 kJ/mol from Cl to Br, but about 100–130 kJ mol^{-1} from Br to I, for a given series. For a given halide, the trend in BDEs is 3 ≈ 4 < 2 < 1, which is nearly according to the stability of the corresponding alkyl free radical generated. The increase is more as we go from 2 to 1 series than going from 3 to 2 series. For a given series of halides, the BDEs decreases while the corresponding C–X bond distance increases (Table 1) as we go from X = Cl to X = I. The BDEs correlates well with the C–X bond lengths; as the C–X bond length increases, BDEs decreases. This plot is presented in Figure 2. Solvent polarity has different effect for 1° alkyl halides (series 1) than those of others (2° and 3°) alkyl halides. The trends are gas phase > anisole > acetonitrile for 2, 3 and 4 series while it is gas phase < anisole < acetonitrile, for series 1 alkyl halides. Thus with increasing polarity of the medium, the relatively-stable radicals (2, 3 and 4 series) become more unstable, while the less stable radicals 1° become more stable.

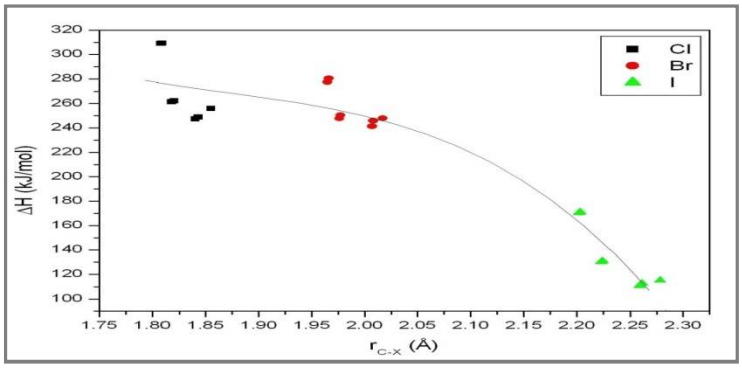

Figure 2. Correlation plot of bond dissociation enthalpies with C–X bond distances of the studied alkyl halides.

Table 2. Enthalpy and Free energy for homolytic cleavage of studied alkyl halides in gas phase, and solution phase

R-X	ΔH (kJ mol^{-1})			ΔG (kJ mol^{-1})		
	Gas phase	Anisole	Acetonitrile	Gas phase	Anisole	Acetonitrile
1a-Cl	303.70	309.05	312.57	262.45	267.16	269.93
1a-Br	277.64	282.13	285.29	237.08	241.09	243.24
1a-I	170.34	173.73	176.57	170.34	133.56	135.65
1b-Cl	304.26	309.43	313.09	263.36	267.38	271.56
1b-Br	280.50	284.99	288.18	239.13	244.36	247.13
1b-I	171.02	174.31	177.18	132.54	135.03	136.56
2a-Cl	263.60	261.46	261.05	223.55	221.94	221.40
2a-Br	247.81	245.20	244.64	207.54	204.98	204.44
2a-I	129.98	127.00	126.20	90.67	88.08	87.14
2b-Cl	264.55	262.34	261.85	224.27	222.55	222.16
2b-Br	250.51	247.83	247.09	209.48	207.32	206.87
2b-I	131.02	127.88	127.13	91.33	87.53	87.61
3a-Cl	250.80	247.48	246.52	208.42	205.48	204.29
3a-Br	241.53	237.68	236.34	198.29	194.46	193.59
3a-I	110.83	106.19	104.63	69.42	64.54	63.12
3b-Cl	252.37	249.04	247.96	210.12	207.74	206.62
3b-Br	245.88	242.06	240.66	203.04	199.95	198.49
3b-I	112.68	107.99	106.35	71.27	68.48	66.05
4-Cl	257.07	255.98	255.53	209.90	208.81	205.31
4-Br	247.87	246.44	245.90	200.87	199.29	195.68
4-I	115.16	112.71	111.66	69.30	66.64	62.98

The free energies for the studied halides (Table 2) are nearly a constant difference with the enthalpy data (about 40 kJ mol^{-1} for series 1, 2, 3 and about 48 kJ mol^{-1} for series 4). This means that the entropy factor contributing for the series 1, 2 and 3 alkyl halides (and similarly for the series 4) is nearly same. This is understandable from the structural similarities among alkyl halides of series 1, 2 and 3, (and similarly series 4). The free energies vary according to $4 \approx 3 < 2 < 1$ for a given X and follows the trends Cl > Br > I for a given series. The free energies like BDEs, increase with decreasing C–X bond lengths and this is plotted in figure 3. Consequently, the correlation between free energies and enthalpies of C–X bond is direct (Figure 4). Calculations in presence of polar solvents show the variation of free energies following the trends, gas phase > anisole > acetonitrile for 2, 3 and 4 series, while the trend becomes gas phase < anisole < acetonitrile for series **1** alkyl halides. This trend is similar to the trends found in BDEs.

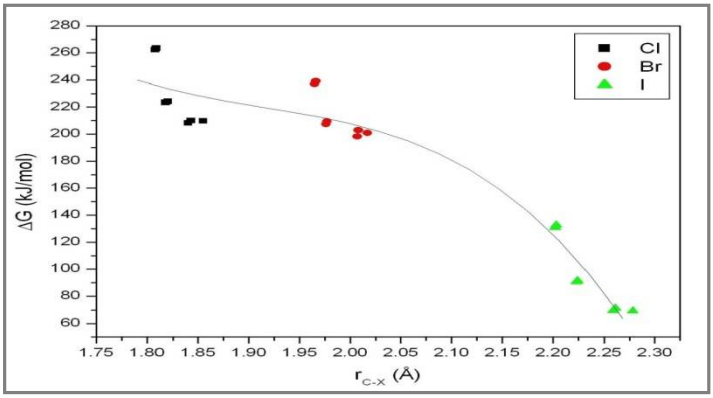

Figure 3. Correlation plot of the free energies with C–X bond distances for the studied alkyl halides.

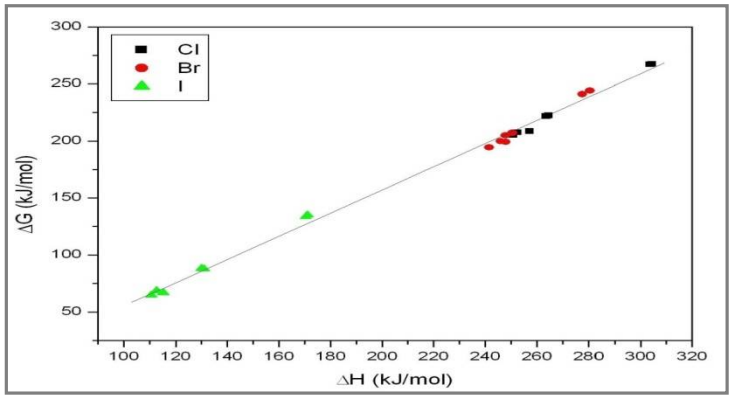

Figure 4. Variation of enthalpies with the free energies for the C–X bond dissociation process for the studied alkyl halides.

Relative Equilibrium Constants (K_{ATRP}): As discussed in introduction, the overall equilibrium constant (K_{ATRP}) can be given as product of two equilibrium constants K_{RX} and K_X, the later depends on catalytic system and halogen radical. Thus, for a given catalytic system and a given X, K_X will be a constant, and relative value of K_{ATRP} can be obtained from knowledge of K_{RX}. We calculate K_{RX} from the free energy. The estimated K_X (= K_{ATRP} / K_{RX}) values for the series 4 alkyl halides from their experimentally determined K_{ATRP} values (1.50×10^{-6} for 4-Cl [**13**], 3.93×10^{-9} for 4-Br [**15**] and 2.2×10^{-8} this for methyl-2-iodopropanoate [**13**]) and then use this K_X value for the rest of the compounds of a given X. The values of K_{ATRP}, so obtained, are displayed in table 3. A quick glance at table 3 shows that the values of K_{ATRP} for the studied alkyl halides differ in orders of magnitude (10^{-4} to 10^{-18} for gas

phase). All the alkyl halides of series 3 and many from series 2 (2a-Cl, 2a-I, 2b-Cl and 2b-I) have comparable K_{ATRP} with those of corresponding commercial initiators (series 4). However, the alkyl halides of series 1 have K_{ATRP} values much smaller than those of series 4 alkyl halides. The K_{ATRP} data follow trends 4 ≈ 3 > 2 >> 1 for a given X, and Cl < Br < I, for a given series. The trends of K_{ATRP} in changing medium of the system are gas phase > anisole > acetonitrile for series 1 alkyl halides, and gas phase < anisole < acetonitrile for the rest of the halides (series 2, 3 and 4). With increasing temperature from 25°C to 80°C, there is order of magnitude increases (10^3 to 10^9) in the values of K_{ATRP}. The good correlation in the variation of K_{ATRP} and C–X bond lengths as well as variation of K_{ATRP} with BDEs has been obtained. These correlation plots are displayed in Figure 5 and 6, respectively. Figure 5 implies that, as the C–X bond length increases -logK_{ATRP} decreases, i.e. logK_{ATRP} increases. This is because as the C–X bond length increases (weak bond) homolysis is easier and so K_{ATRP} increases. Thus, iodides are better initiators than bromides which in turns better initiators than chlorides. However, for a given X the variation of C–X bond length is very little, yet there is an order of magnitude difference in K_{ATRP}. This is mainly due to the structural difference (primary, secondary, tertiary) of alkyl halides. A similar explanation holds for the correlations between BDEs and K_{ATRP} of figure 6.

Table 3. Relative values of K_{ATRP} for homolytic bond cleavage of studied alkyl halides in gas phase and in solution phase at 25°C and 80°C

R-X	K_{ATRP} at 25°C			K_{ATRP} at 80°C		
	Gas	Anisole	Acetonitrile	Gas	Anisole	Acetonitrile
1a-Cl	9.34×10^{-16}	8.98×10^{-17}	7.20×10^{-18}	1.85×10^{-07}	2.48×10^{-08}	2.13×10^{-09}
1a-Br	1.78×10^{-15}	1.88×10^{-16}	1.83×10^{-17}	6.83×10^{-08}	9.44×10^{-09}	9.79×10^{-10}
1a-I	1.26×10^{-15}	1.69×10^{-16}	5.70×10^{-17}	5.68×10^{-11}	9.17×10^{-12}	3.84×10^{-12}
1b-Cl	6.46×10^{-16}	8.23×10^{-17}	3.70×10^{-18}	1.32×10^{-07}	2.11×10^{-08}	1.52×10^{-09}
1b-Br	7.77×10^{-16}	5.00×10^{-17}	3.82×10^{-18}	3.56×10^{-08}	3.07×10^{-09}	3.30×10^{-10}
1b-I	6.31×10^{-16}	9.31×10^{-17}	3.90×10^{-17}	2.97×10^{-11}	5.55×10^{-12}	3.22×10^{-12}
2a-Cl	6.10×10^{-09}	7.50×10^{-09}	2.30×10^{-09}	9.60×10^{-02}	9.07×10^{-02}	3.04×10^{-02}
2a-Br	1.97×10^{-11}	3.97×10^{-10}	1.15×10^{-10}	1.55×10^{-03}	1.95×10^{-03}	5.48×10^{-04}
2a-I	1.37×10^{-08}	1.56×10^{-08}	1.80×10^{-08}	4.84×10^{-05}	4.58×10^{-05}	4.88×10^{-05}
2b-Cl	4.56×10^{-09}	5.86×10^{-09}	1.70×10^{-09}	7.61×10^{-02}	8.59×10^{-02}	2.36×10^{-02}
2b-Br	1.22×10^{-10}	1.54×10^{-10}	4.32×10^{-11}	8.38×10^{-04}	8.98×10^{-04}	2.41×10^{-04}
2b-I	1.05×10^{-08}	1.96×10^{-08}	1.50×10^{-08}	3.96×10^{-05}	6.25×10^{-05}	4.38×10^{-05}
3a-Cl	2.73×10^{-06}	5.75×10^{-06}	1.00×10^{-06}	$1.92\times10^{+01}$	$3.29\times10^{+01}$	5.27
3a-Br	1.11×10^{-08}	2.76×10^{-08}	9.16×10^{-09}	4.34×10^{-02}	8.52×10^{-02}	2.59×10^{-02}
3a-I	7.23×10^{-05}	2.08×10^{-04}	2.90×10^{-04}	7.65×10^{-02}	1.62×10^{-01}	2.07×10^{-01}
3b-Cl	1.37×10^{-06}	2.31×10^{-06}	8.80×10^{-07}	$1.06\times10^{+01}$	$1.45\times10^{+01}$	5.27
3b-Br	1.63×10^{-09}	3.02×10^{-09}	1.27×10^{-09}	6.72×10^{-03}	1.23×10^{-02}	4.73×10^{-03}
3b-I	3.43×10^{-05}	4.25×10^{-05}	8.80×10^{-05}	4.07×10^{-02}	3.90×10^{-02}	7.04×10^{-02}
4-Cl	1.50×10^{-06}	1.50×10^{-06}	1.50×10^{-06}	$1.56\times10^{+01}$	$1.46\times10^{+01}$	$1.27\times10^{+01}$
4-Br	3.93×10^{-09}	3.93×10^{-09}	3.93×10^{-09}	2.29×10^{-02}	2.09×10^{-02}	1.81×10^{-02}
4-I	7.59×10^{-05}	8.93×10^{-05}	3.10×10^{-04}	1.05×10^{-01}	1.07×10^{-01}	4.67×10^{-01}

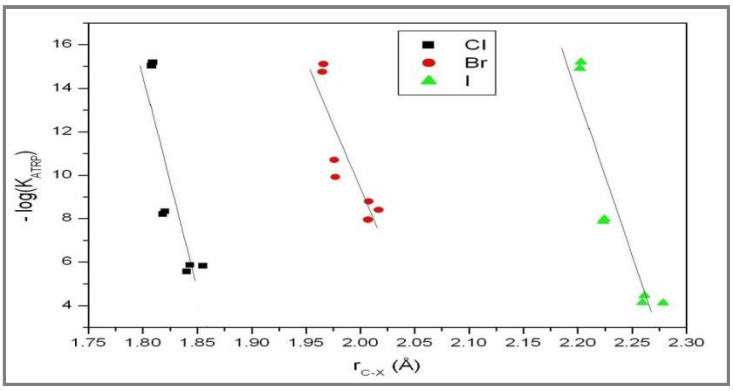

Figure 5. Correlation plot of relative K_{ATRP} with C–X bond lengths for the studied alkyl halides.

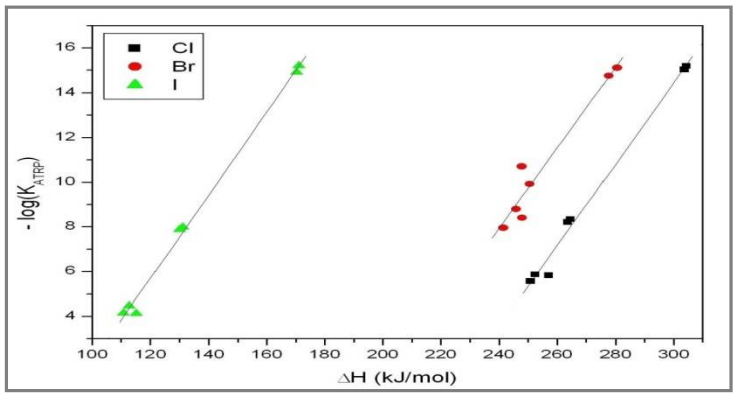

Figure 6. Correlation plot of relative K_{ATRP} values with R–X bond enthalpies of studied alkyl halides.

APPLICATION

The chosen study helps us to synthesize the initiators (structurally similar to *N*-arylitaconimide monomer) in the laboratory for the copolymerization of *N*-arylitaconimides and methyl methacrylate using ATRP process. The designed initiators will be helpful for the synthesis of various functional polymers of *N*-arylitaconimide monomers. These polymers can be useful for the high temperature service [**36**].

CONCLUSION

The structural and thermodynamic properties (bond dissociation enthalpies and free energies) of a series of alkyl halides having structural similarities with substituted itaconimides along with some common ATRP initiators have been reported. Relative values of K_{ATRP} are extracted from the free energy values with respect to common ATRP initiators. Variations of different properties with system parameters are studied. As expected, the C–X bond lengths increase in the order Cl < Br < I for a given R and 4 ≈ 3 < 2 < 1 for a given X, while the BDEs, and free energies follow the opposite trends. With increase in the polarity of the medium, the C–X bond distances increase (BDEs and free energies decreases) for series 2, 3 and 4, while opposite trend is observed for series 1 (Primary) alkyl halides. The value of K_{ATRP} for series 3 and many alkyl halides of series 2 are comparable to those of common ATRP initiators. Thus alkyl halides of series 3 and some of series 2 (2a-Cl, 2a-I, 2b-Cl and 2b-I) have potential to initiate ATRP process, and worth investigating further. Additionally, it is also found that values of K_{ATRP} slightly decrease with increasing solvent polarity and increase significantly with increasing temperature.

ACKNOWLEDGEMENT

I thank to Prof. R. N. Behera and Dr. Rashmi Chauhan, Department of Chemistry, BITS, Pilani - K. K. Birla Goa Campus for their support to carry out this work. The use of DST-FIST computational facility of the Department of Chemistry, BITS, Pilani - K. K. Birla Goa Campus is gratefully acknowledged.

REFERENCES

[1]. J. S. Wang, K. Matyjaszewski, Controlled/"living" radical polymerization, atom transfer radical polymerization in the presence of transition-metal complexes, *J. Am. Chem. Soc.*, **1995**, 117, 5614-5615.

[2]. M. Kato, M. Kamigaito, M. Sawamoto, T. Higashimura, Polymerization of methylmethacrylate with the carbon tetrachloride/dichlorotris- (triphenylphosphine)ruthenium(II) /Methylaluminum

Bis(2,6-di-tert-butylphenoxide) initiating system: Possibility of living radical polymerization, *Macromolecules*, **1995**, 28, 1721-1723.
[3]. K. Matyjaszewski, J. Xia, Atom transfer radical polymerization, *Chem. Rev.*, **2001**, 101, 2921-2990.
[4]. M. Kamigaito, T. Ando, M. Sawamoto, Metal-catalyzed living radical polymerization, *Chem. Rev.*, **2001**, 101, 3689-3746.
[5]. K. Matyjaszewski, Ed. Controlled/living radical polymerization, from synthesis to materials; ACS Symposium Series 944; American Chemical Society: Washington, DC, **2006**.
[6]. A. D. Jenkins, R. G. Jones, G., Moad, Terminology for reversible-deactivation radical polymerization previously called "controlled" radical or "living" radical polymerization (IUPAC Recommendations 2010), *Pure. Appl. Chem.*, **2010**, 82, 483-491.
[7]. N. V. Tsarevsky, K. Matyjaszewski, "Green" atom transfer radical polymerization: from process design to preparation of well-defined environmentally friendly polymeric materials, *Chem. Rev.*, **2007**, 107, 2270-2299.
[8]. K. Matyjaszewski, Atom transfer radical polymerization (ATRP): Current status and future perspectives, *Macromolecules*, **2012**, 45, 4015-4039.
[9]. K. Matyjaszewski, Ed. Controlled/Living radical polymerization, progress in ATRP, NMP, and RAFT; ACS Symposium Series 768; American Chemical Society: Washington, DC, **2000**.
[10]. C. J. Hawker, A. W. Bosman, E. Harth, New polymer synthesis by nitroxide mediated living radical polymerizations, *Chem. Rev.*, **2001**, 101, 3661-3688.
[11]. C. Barner-Kowollik, T. P. Davis, J. P. Heuts, M. H. Stenzel, P. Vana, M. Whittaker, RAFTing down under: Tales of missing radicals, fancy architectures, and mysterious holes, *J. Polym. Sci., Part A: Polym. Chem.*, **2003**, 41, 365-375.
[12]. W. A. Braunecker, K. Matyjaszewski, Controlled/living radical polymerization: Features, developments, and perspectives, *Prog. Polym. Sci.*, **2007**, 32, 93-146.
[13]. Controlled and Living Polymerization, ed. A. H. E. Muller, K. Matyjaszewski, WILEY-VCH Verlag GmbH & Co. KGaA, Weinheim, **2009**.
[14]. T. Pintauer, P. Zhou, K. Matyjaszewski, General method for determination of the activation, deactivation, and initiation rate constants in transition metal-catalyzed atom transfer radical processes, *J. Am. Chem. Soc.*, **2002**, 124, 8196-8197.
[15]. W. Tang, N. V. Tsarevsky, K. Matyjaszewski, Determination of equilibrium constants for atom transfer radical polymerization, *J. Am. Chem. Soc.*, **2006**, 128, 1598-1604.
[16]. W. Tang, Y. Kwak, W. Braunecker, N. V. Tsarevsky, M. L. Coote, K. Matyjaszewski, Understanding atom transfer radical polymerization: Effect of ligand and initiator structures on the equilibrium constants, *J. Am. Chem. Soc.*, **2008**, 130, 10702-10713.
[17]. D. A. Singleton, D. T. Nowlan, N. Jahed, K. Matyjaszewski, Isotope effects and the mechanism of atom transfer radical polymerization, *Macromolecules*, **2003**, 36, 8609-8616.
[18]. I. Degirmenci, S. Eren, V. Aviyente, Modeling the solvent effect on the tacticity in the free radical polymerization of methyl methacrylate, *Macromolecules*, **2010**, 43, 5602-5610.
[19]. A. P. Haehnel, M. Schneider-Baumann, K. U. Hiltebrandt, A. M. Misske, C. Barner-Kowollik, Global trends for k_p? Expanding the frontier of ester side chain topography in acrylate and methacrylates, *Macromolecules*, **2013**, 46, 15-28.
[20]. M. L. Coote, Quantum-chemical modeling of free-radical polymerization, *Macromol. Theory. Simul.*, **2009**, 18, 388-400.
[21]. M. D. Miller, A. J. Holder, A quantum mechanical study of methacrylate free-radical polymerizations, *J. Phys. Chem.*, **2010**, A 114, 10988-10996.
[22]. H. Fischer, The persistent radical effect: A principle for selective radical reactions and living radical polymerizations, *Chem. Rev.*, **2001**, 101, 3581-3610.
[23]. A. Goto, T. Fukuda, Kinetics of living radical polymerization, *Prog. Polym. Sci.*, **2004**, 29, 329-385.
[24]. H. Fischer, The persistent radical effect in controlled radical polymerizations, *J. Polym. Sci., Part A: Polym. Chem.*, **1999**, 37, 1885-1901.

[25]. W. Tang, Y. Kwak, W. Braunecker, N. V. Tsarevsky, M. L. Coote, K. Matyjaszewski, Understanding atom transfer radical polymerization: Effect of ligand and initiator structures on the equilibrium constants, *J. Am. Chem. Soc.*, **2008**, 130, 10702-10713.
[26]. M. B. Gillies, K. Matyjaszewski, P-O. Norrby, T. Pintauer, R. Poli, P. Richard, A DFT study of r-x bond dissociation enthalpies of relevance to the initiation process of atom transfer radical polymerization, *Macromolecules*, **2003**, 36, 8551-8559.
[27]. C. Y. Lin, M. L. Coote, A. Gennaro, K. Matyjaszewski, Ab initio evaluation of the thermodynamic and electrochemical properties of alkyl halides and radicals and their mechanistic implications for atom transfer radical polymerization, *J. Am. Chem. Soc.*, **2008**, 130, 12762-12774.
[28]. T. Guliashvili, V. Percec, A comparative computational study of the homolytic and heterolytic bond dissociation energies involved in the activation step of ATRP and SET-LRP of vinyl monomers, *J. Polym. Sci., Part A: Polym. Chem.*, **2007**, 45, 1607-1618.
[29]. C. Y. Lin, S. R. A. Marque, K. Matyjaszewski, M. L. Coote, Linear-free energy relationships for modeling structure reactivity trends in controlled radical polymerization, *Macromolecules*, **2011**, 44, 7568-7583.
[30]. K. P. Patel, M. I. Shekh, Synthesis and investigation of chemically modified Phthalimide based copolymers and their Antimicrobial activity, *J. Applicable Chem.*, **2013**, 2, 902-912.
[31]. B. J. Khairnar, P. S. Girase, D. V. Mane, B. R. Chaudhari, Polymer Supported DABCO as an Eco-Friendly and Green Catalyst for Synthesis of 2-arylbenzothiazole in Aqueous Media, *J. Applicable Chem.*, **2019**, 8, 1783-1789.
[32]. B. J. Khairnar, P. S. Girase, B. R. Chaudhari, Facile and Green Syntheses of Substituted-5-arylidene-2,4-thiazolidinediones using Polymer Supported DABCO as an Eco-Friendly Catalyst in Aqueous Medium, *J. Applicable Chem.*, **2019**, 8, 565-573.
[33]. A. Pandey, K. P. Tiwari, Electrochemical Polymerization and Characterization of Multipurpose Advanced Polymers, *J. Applicable Chem.*, **2020**, 9, 447-450.
[34]. R. Chuahan, V. Choudhary, Copolymerization of *N*-(4-Carboxyphenyl) itaconimide or *N*-(4-carboxyphenyl) itaconamic acid with methyl methacrylate, *J. Appl. Polym. Sci.*, **2005**, 98, 1909-1915.
[35]. R. Chuahan, V. Choudhary, Thermal and mechanical properties of copolymers of methyl methacrylate with *N*-aryl itaconimides, *J. Appl. Polym. Sci.*, **2009**, 112, 1088-1095.
[36]. C. Deoghare, V. S. Nadkarni, R. N. Behera, R. Chauhan, Synthesis and Characterization of Copolymers of Methyl Methacrylate with *N*-arylitaconimides via AGET-ATRP, *J. Polym. Mater.*, **2017**, 34, 455-466.
[37]. Gaussian Revision B., M. J. Frisch, G. W. Trucks, H. B. Schlegel, G. E. Scuseria, M. A. Robb, J. R. Cheeseman, G. Scalmani, V. Barone, B. Mennucci, G. A. Petersson, H. Nakatsuji, M. Caricato, X. Li, H. P. Hratchian, A. F. Izmaylov, J. Bloino, G. Zheng, J. L. Sonnenberg, M. Hada, M. Ehara, K. Toyota, R. Fukuda, J. Hasegawa, M. Ishida, T. Nakajima, Y. Honda, O. Kitao, H. Nakai, T. Vreven, J. A. Montgomery, Jr., J. E. Peralta, F. Ogliaro, M. Bearpark, J. J. Heyd, E. Brothers, K. N. Kudin, V. N. Staroverov, T. Keith, R. Kobayashi, J. Normand, K. Raghavachari, A. Rendell, J. C. Burant, S. S. Iyengar, J. Tomasi, M. Cossi, N. Rega, J. M. Millam, M. Klene, J. E. Knox, J. B. Cross, V. Bakken, C. Adamo, J. Jaramillo, R. Gomperts, R. E. Stratmann, O. Yazyev, A. J. Austin, R. Cammi, C. Pomelli, J. W. Ochterski, R. L. Martin, K. Morokuma, V. G. Zakrzewski, G. A. Voth, P. Salvador, J. J. Dannenberg, S. Dapprich, A. D. Daniels, O. Farkas, J. B. Foresman, J. V. Ortiz, J. Cioslowski, and D. J. Fox, Gaussian, Inc., Wallingford CT, (**2010**).
[38]. C. Lee, W. Yang, R. G. Parr, Development of the Colle-Salvetti correlation-energy formula into a functional of the electron density, *Phys. Rev.*, **1988**, B37, 785-789.
[39]. A. D. Becke, Density-functional exchange-energy approximation with correct asymptotic behavior, *Phys. Rev.*, **1988**, A38, 3098-3100.
[40]. A. D. Becke, Density-functional thermochemistry. III. The role of exact exchange, *J. Chem. Phys.*, **1993**, 98, 5648-5653.

[41]. C. E. Moore, Atomic Energy Levels, US Government Printing Office, Washington, DC, **1952**, Vols. I-III.
[42]. S. Miertus, E. Scrocco, J. Tomasi, Electrostatic interaction of a solute with a continuum. A direct utilization of *Ab* initio molecular potentials for the prevision of solvent effects, *Chem. Phys.*, **1981**, 55, 117-129.